A Spectroscopic Investigation of Cerium Molybdenum Oxides †

Tery L. Barr and Charles G. Fries
UOP Corporate Research Center, Ten UOP Plaza, Des Plaines, Illinois 60016, U.S.A.
Franco Cariati
Instituto di Chimica Generale, Università di Sassari, Via Vienna 2, Sassari, Italy
Jan C. J. Bart *
Department of Metallurgy and Science of Materials, University of Oxford, Parks Road, Oxford OX1 3PH
Nicola Giordano
Istituto di Chimica Industriale, Università di Messina, Messina, Italy

A detailed *X*-ray photoelectron, i.r., and Raman spectral study has been made of $Ce_2(MoO_4)_3$ and five novel cerium molybdenum oxides (α- and β-$Ce_2Mo_4O_{15}$, β- and γ-$Ce_2Mo_3O_{13}$, and $Ce_8Mo_{12}O_{49}$), which are of particular interest as they are closely related to the cerium molybdenum oxide species which are expected to play an active role in an industrial cerium molybdenum tellurium oxide acrylonitrile catalyst. The photoemission results add to the few existing previous data concerning cerium compounds and confirm the valence distribution in the compounds. With the exception of the tetrahedral oxomolybdenum co-ordination in $Ce_2(MoO_4)_3$ the cerium molybdates consist of highly irregular or mixed polyhedral arrangements with Mo–O bond strengths (in valence units) either below 0.3 v.u or above 1.0 v.u.

Although cerium molybdates are used as such [1] or in combination to other oxides as components in an industrial catalyst system for selective ammoxidation of propylene,[2,3] relevant structural information is scarce. Only the very complex phase relationships in the cerium molybdenum oxide system have been worked out to a considerable extent and the main present knowledge is contained in refs. 4—9. We have now undertaken an extensive study by means of i.r., Raman, and x.p. (*X*-ray photoelectron) spectroscopy on some of these novel cerium molybdenum oxide compounds,[10] namely $Ce_2Mo_3O_{13}$, $Ce_2Mo_4O_{15}$, and $Ce_8Mo_{12}O_{49}$ as well as the much earlier described scheelite, $Ce_2(MoO_4)_3$. The work was supported by extensive x.p.s. studies of other cerium and molybdenum systems, in particular the elemental metal foils. This type of support is useful since only a few previous electron spectroscopy studies of Ce systems have been published [11–15] and no previous reports exist of the combined systems. Similarly, the i.r. and Raman studies have been conducted by comparison to other molybdates of known structure.

Experimental

Materials.—The cerium molybdenum oxides were original samples; [6] CeO_2 was prepared by calcination of $Ce(NO_3)_3 \cdot 6H_2O$ at 600 °C. Metal foils of Mo and Ce were available as thin, high-purity materials (McKay). Support materials Ce_2O_3 and MoO_3 were in the form of passivated Ce and Mo foils. The cerium molybdenum oxides and CeO_2 were examined as powders which were pressed into thin wafers using a special die.

Apparatus.—*X*-Ray photoelectron spectroscopy (x.p.s.) measurements were carried out on a HP-5950 A spectrometer operated at 10^{-9} Torr and 300 K. The Mo(3*p*, 3*d*), Ce(3*p*, 3*d*, 4*d*), and O(1*s*) spectra were collected under high-resolution conditions (pass energy = 20—50 eV), using the Al-K_α source at a power of 800 W. As most of the materials examined were insulators, charge shifts were removed using a HP 18623 Electron Flood Gun operated at 0.5 mA. Several of the species were subjected to sputter etching with a Physical Electronics Sputtering Gun in the x.p.s. sample preparation chamber in order to remove the contaminated outer surface layer and to take advantage of the tendency of some of the principal elements to undergo reduction in the Ar^+ ion beam of the sputtering gun.[16] Generally, an Ar gas pressure of 5×10^{-5} Torr was maintained throughout the etching experiments.

The data were analyzed using a non-linear least-squares computer program in which the background was approximated by a sloping straight line. The free parameters were the line position and amplitude, the linewidth and the background position and slope. The deconvolution was performed on a HP 2100 A computer.

Infrared and Raman spectra were recorded using a Beckman model 4250 and a Coderg PHO spectrophotometer, respectively, using KBr pellets in the former case.

Results and Discussion

Photoelectron Spectra.—Preliminary analysis by means of a 1 000 eV scan of the cerium molybdenum oxide samples indicated high purity with traces of carbon [x.p.s. C(1*s*) absorption at 284.7 eV].

The binding energies of the principal peaks of the constituents of the samples and the support materials are given in Table 1. In view of the fact that various materials are experiencing variable charge shifts which are removed with different flood gun settings and as insulators do not have a true Fermi level, the absolute determination of binding energies is difficult for these species. The variability of the C(1*s*) binding energies is typical in this respect. Data reported are calibrated to C(1*s*) = 284.7 eV.

The peak position of the O(1*s*) spectra (*ca.* 529.2 eV) is characteristic of metallic oxides. However, it is impossible to distinguish between anions belonging to the molybdenum and cerium co-ordination spheres. A frequently observed slight shoulder on the high binding energy side is due to chemisorbed oxygen.

The Mo(3*d*) binding energy of β-$Ce_2Mo_4O_{15}$ [Figure 1(*a*)] differs from that of MoO_3 on the surface of Mo foil [Figure 1(*e*); note the small Mo^0 peak at *ca.* 228 eV]. This does not indicate differences in oxidation states but merely reflects the Fermi edge problem mentioned above. The measured Mo binding energies are invariably characteristic of the +6 oxidation state.

The individual Ce peaks are the most revealing part of the

† *Non-S.I. units employed:* eV ≈ 1.60×10^{-19} J; Torr = (101 325)/760 Pa.

Table 1. Binding energies and linewidths (l.w.) in eV for cerium molybdates and related systems (±0.1 eV) [a]

		γ-$Ce_2Mo_3O_{13}$	β-$Ce_2Mo_3O_{13}$	α-$Ce_2Mo_4O_{15}$ [b]	β-$Ce_2Mo_4O_{15}$	$Ce_8Mo_{12}O_{49}$	$Ce_2(MoO_4)_3$	CeO_2	Ce_2O_3 (foil)	MoO_3 (foil)
Mo($3d_{\frac{5}{2}}$)		232.30	232.55	232.46 (233.65)	232.45	232.52	232.3			232.66
	l.w.	1.42	1.38	1.18	1.18	1.47	1.9			1.20
Mo($3d_{\frac{3}{2}}$)		235.47	235.73	235.59	235.59	235.68	23.54			235.75
Mo($3p_{\frac{3}{2}}$)		397.90	398.10	398.13	398.18	398.08	39.81			398.43
Ce($3d_{\frac{5}{2}}$)	Prin	882.30	882.39	882.15	882.20	882.45	88.16	881.83	880.60	
	Sat. 1			806.05	885.50	885.65	88.54		884.80	
Ce($3d_{\frac{3}{2}}$)	Prin.	900.88	900.82	900.55	900.70	901.05	90.08	900.40	899.20	
	Sat. 1			904.25 (904.95)	904.30	904.65	90.45		903.40	
	Sat. 2	898.25	898.31			898.65		897.90		
	Sat. 3	916.65	916.70			917.00		916.25		
Ce(4d)		108.35	108.51	109.35	108.80	108.50	10.86	107.90	107.60	
		111.80	111.90	111.35	111.20	112.00	11.19	111.44	110.70	
			121.87			121.95		121.28		
			125.05			125.25		124.63		
O(1s)		529.58	529.64	530.19	530.17	529.83	529.9	528.60	528.90	530.52
	l.w.	1.54	1.65	1.44	1.42	1.70	2.0	1.05	1.16	1.70 [c]

[a] Calibrated at C(1s) = 284.7 eV; prin. = principle peak, sat. = satellite. [b] Values in parentheses refer to results of sputter etching. [c] Extensive adsorbed O_2 and hydroxide impurity.

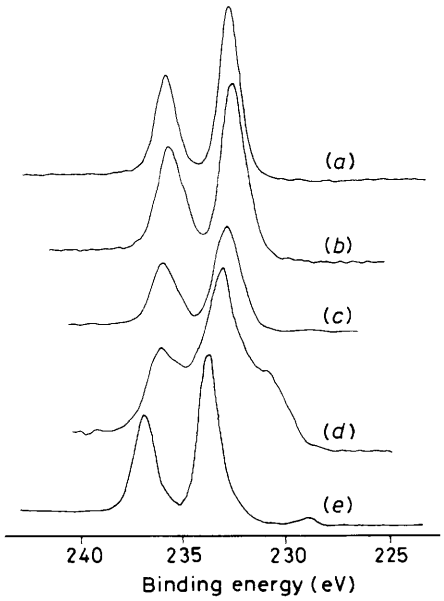

Figure 1. Mo(3d) photoemission spectra of β-$Ce_2Mo_4O_{15}$ (*a*), γ-$Ce_2Mo_3O_{13}$ (*b*), $Ce_8Mo_{12}O_{49}$ (*c*), α-$Ce_2Mo_4O_{15}$ after sputtering for 2 min (*d*), and MoO_3 on Mo foil (*e*)

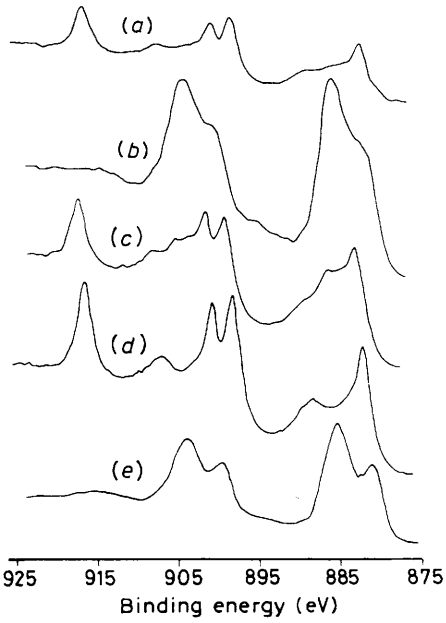

Figure 2. Ce(3d) photoemission spectra of β-$Ce_2Mo_3O_{13}$ (*a*), α-$Ce_2Mo_4O_{15}$ (*b*), $Ce_8Mo_{12}O_{49}$ (*c*), CeO_2 (*d*), and Ce_2O_3 on Ce foil (*e*)

x.p. spectra. The Ce(3d) region of β-$Ce_2Mo_3O_{13}$ [Figure 2(*a*)] displays an intricate complexity of the satellite structure, which arises from a complex mixture of multielectron and multiplet interactions. The observed approximate mirror plane at *ca.* 900 eV is due to spin-orbit splitting. Quite similar results were found for γ-$Ce_2Mo_3O_{13}$. One of the key peaks of analysis of the Ce(3d) region of cerium molybdenum oxides is the $3d_{\frac{3}{2}}$ satellite at *ca.* 917 eV. Comparison of the 875—925 eV scan for CeO_2 [Figure 2(*d*)] with β- and γ-$Ce_2Mo_3O_{13}$ shows the presence of Ce^{IV} in the latter. In case of β-$Ce_2Mo_3O_{13}$ this is further confirmed by comparison with the Ce(4d) region of CeO_2 [Figure 3(*a*) and (*c*)]. As to the details of the spectra, we notice that some Mo^{V} and Ce^{III} are present in the $Ce_2Mo_3O_{13}$ polymorphs. Molybdenum(v) is detected by the increased linewidth, as compared to the $Ce_2Mo_4O_{15}$ compounds. Some evidence for small amounts of Ce^{III} is also found by careful examination of the Ce(3d, 4d) spectra for β- and γ-$Ce_2Mo_3O_{13}$, namely by the small lumps around the binding energy regions at 884 and 904 eV [Figure 2(*a*)]; the structure in this region is due to the principal satellite of the $3d_{\frac{5}{2}}$ and $3d_{\frac{3}{2}}$ lines of Ce^{III}. This is further reflected by the lack of ' total ' growth of the Ce(4d) satellites for β-$Ce_2Mo_3O_{13}$ as compared to CeO_2. The Ce^{IV} satellite structure in the 120—125 eV region is of about equal intensity as the main branch (105—115 eV), whereas the high binding energy satellites are noticeably larger for CeO_2 [Figure 3(*c*)]. It should be noted that there is as yet no absolute proof for the exclusive nature of these satellites. In fact, there appears to be evidence that Ce^{III} and Ce^{IV} share some multielectron satellites for certain classes of anions. It is also known that different anions bonded to Ce will generate different structures for the resulting multielectron satellites. Thus, one should expect a molybdate to produce some

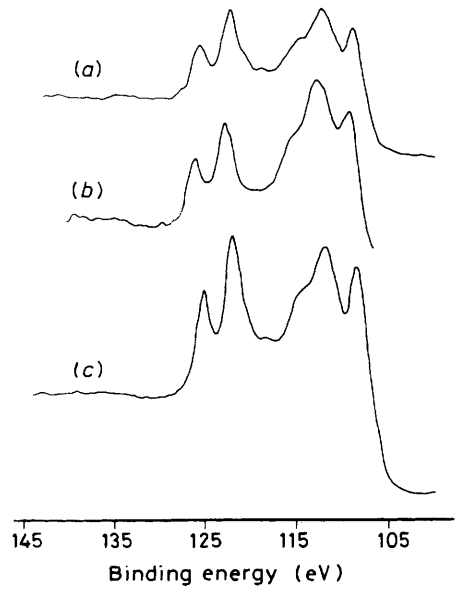

Figure 3. Ce(4*d*) photoemission spectra of β-$Ce_2Mo_3O_{13}$ (*a*), $Ce_8Mo_{12}O_{49}$ (*b*), and CeO_2 (*c*)

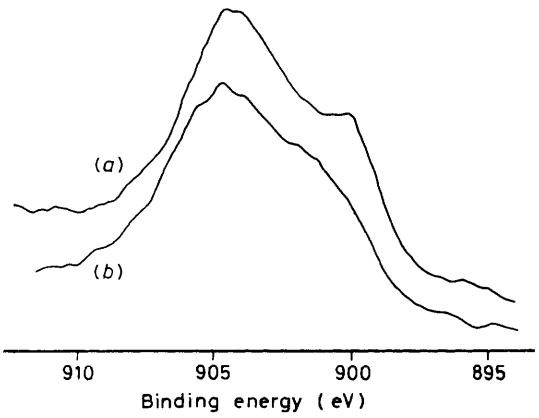

Figure 4. Ce($3d_{\frac{5}{2}}$) photoemission spectra of β-$Ce_2Mo_4O_{15}$ (*a*), and α-$Ce_2Mo_4O_{15}$ after sputtering for 2 min (*b*)

variation from an oxide. Even considering these features, we feel that the Ce^{IV} compounds contain very small amounts of Ce^{III}, typically of the order of 1%. This may eventually be on account of surface degradation rather than the preparative conditions.

A scan for α-$Ce_2Mo_4O_{15}$ in the Ce(3*d*) spectral range [Figure 2(*b*)] shows a marked change in satellite structure with the principal peak at about the same binding energy but without an absorption at 916.5 eV. A narrow scan examination of the Ce($3d_{\frac{5}{2}}$) region for β-$Ce_2Mo_4O_{15}$ [Figure 4(*a*)] shows similar features as for α-$Ce_2Mo_4O_{15}$. In both cases, the similarity with the Ce_2O_3 spectrum obtained by sputter removal of the Ce^{IV} layer on a Ce foil [Figure 2(*e*)] is quite striking. Consequently, the analysis for α- and β-$Ce_2Mo_4O_{15}$ with their extremely narrow x.p.s. linewidths is in accordance with the presence of Ce^{III}, Mo^{VI}, and a typical 'oxide' O(1*s*) and conforms to the expectations. The small rise in the spectra of the $Ce_2Mo_4O_{15}$ compounds at *ca.* 916.5 eV is interpreted as being due to weak Ce^{III} satellites rather than Ce^{IV} impurities. This conclusion is supported by the lack of evidence for satellites in the 120—125 eV region.[17]

As to $Ce_8Mo_{12}O_{49}$, x.p.s. evidence [Figures 1(*c*), 2(*c*), and 3(*b*)] is in agreement with a mixed Ce^{III}–Ce^{IV} compound with the Ce^{III} multielectron satellite being visible at 904.6 eV. The Ce(4*d*) spectrum clearly shows the Ce^{IV} satellite above 120 eV and the Ce^{III} satellite at *ca.* 112.0 eV. Although it is difficult to partition Figure 2(*c*), the Ce^{III}–Ce^{IV} ratio was derived by a procedure based on relative peak intensities and requiring a circumlocutory series of ratios in order to cancel indeterminate sensitivity factors. Using this method to analyse the Ce(4*d*) peaks unique to Ce^{IV} we obtained a Ce^{III}–Ce^{IV} ratio of *ca.* 2.8 (theoretical 3.0).

The oxide α-$Ce_2Mo_4O_{15}$, which is a candidate active component of the cerium molybdenum tellurium oxide acrylonitrile catalyst, was sputter etched for 2 min using standard conditions. This was done in relation to the effect of sputter reduction, which is observed for many transition metals subjected to the intense action of Ar^+ ions.[16] This phenomenon has also been reported for Mo and Ce.[16,17] Although Ce^{III} in α-$Ce_2Mo_4O_{15}$ is only marginally affected by sputtering [Figure 4(*b*)], as expected, there is a definite significant binding energy shift for all species (Table 1). This appears to reflect not only a reduction in the oxidation state of molybdenum, but also a degradation of the relatively complex cerium molybdate compounds to simpler oxides (MoO_3, Mo_2O_5, MoO_2, and Ce_2O_3). During sputtering molybdenum was reduced to Mo^{4+} with little or no Mo^0 produced [Figure 1(*d*)]. In similar conditions also the Mo oxides on molybdenum foil reduce to the lowest valent oxide (MoO_2),[16] contrary to some of the molybdenum in the cerium molybdenum tellurium oxide catalyst which reduces to Mo^0.

Vibrational Spectra.—Amongst the reported i.r. spectra the one referring to β-$Ce_2Mo_4O_{15}$ is closest to that of octahedral structures, such as α-$NiMoO_4$[18] and MoO_3,[19] in which Mo–O stretching vibrations are observed in the 700—400 cm^{-1} region (Table 2). In all cases the most intense absorption occurs in the range 800—850 cm^{-1}. Taking into account the relationship between the internal force constants and Mo–O bond strengths (Figure 7 of ref. 19), we deduce that few Mo–O links are present in these compounds with bond strengths in the range 1.0—0.3 v.u. (corresponding to bond lengths of 1.88—2.3 Å). Obviously, this conclusion is valid in so far as vibrational coupling between stretching modes of Mo–O bonds with greatly differing bond strengths is not considered. In this context it is also to be noted that the vibrational frequencies for the very long Mo–O bonds are expected in the spectral range of the δ(O–Mo–O) deformations (400—300 cm^{-1}).[20,21]

It may be seen from Figure 5 that some analogies exist between the Raman spectra of β- and γ-$Ce_2Mo_3O_{13}$ and between those of α- and β-$Ce_2Mo_4O_{15}$. In the $Ce_2Mo_3O_{13}$ polymorphs the most intense Raman bands are in the range 800—700 cm^{-1}, and in the $Ce_2Mo_4O_{15}$ compounds, $Ce_8Mo_{12}O_{49}$ and $Ce_2(MoO_4)_3$ above 900 cm^{-1} (Figure 5). Generally, Raman spectra of compounds with an octahedral oxomolybdenum co-ordination exhibit main absorption bands in the high frequency range (>900 cm^{-1}). This is typically the case in $NiMoO_4$ and $MoO_3 \cdot H_2O$, although there are notable exceptions, such as MoO_3.[19] According to recent work by Fallon and Gatehouse[22] β-$Ce_2Mo_4O_{15}$ contains both tetrahedral and octahedral MoO_4^{2-} species. The complex $Ce_2(MoO_4)_3$, which is isostructural with $La_2(MoO_4)_3$,[23,24] has a distorted tetrahedral oxomolybdenum co-ordination. Infrared and Raman spectra indicate a maximum site symmetry for MoO_4^{2-} of C_{2v}. Whereas at least two Raman active Mo–O stretching vibrations $\nu_1(A_1)$ and $\nu_3(F_2)$ are predicted for a tetrahedral MoO_4^{2-} grouping, and one active i.r. stretching $\nu_3(F_2)$, four ν(Mo–O) stretching bands are observed in the i.r.

Table 2. Infrared (i.r.) and Raman (R) Mo–O stretching frequencies (cm^{-1}) *

γ-$Ce_2Mo_3O_{13}$		β-$Ce_2Mo_3O_{13}$		α-$Ce_2Mo_4O_{15}$		β-$Ce_2Mo_4O_{15}$		$Ce_8Mo_{12}O_{49}$		$Ce_2(MoO_4)_3$	
i.r.	R	i.r.	R	i.r.	R	i.r.	R	i.r.	R	i.r.	R
960w		960w	952w	963m	955s	1 000m		940s	945m	935 (sh)	
940m	930w	925w	923vw	945s	940s	960 (sh)	970w	925 (sh)	920s	915s	918s
900 (sh)			903vw	938 (sh)		935 (sh)	938s	875vs		845vs	
830vs		860 (sh)		930 (sh)		910vs	922m	838vs	835w		824m
800 (sh)	790 (sh)	822vs		922 (sh)	920w		900w	800vs		815vs	
780 (sh)	765s	805 (sh)		910m		885vs		770 (sh)	775vw	721vs	
720m	700m	772s	785 (sh)	890s	890w	825vs	835m,br	732m			
			765vs	840vs	840m	760 (sh)		722 (sh)			
		745 (sh)	752vs	828 (sh)	820m	650m		697 (sh)	690w		
			730 (sh)	803s		570m					
				760s	750w,br						
				730s							
				710 (sh)							

* w = Weak, m = medium, s = strong, v = very, sh = shoulder, br = broad.

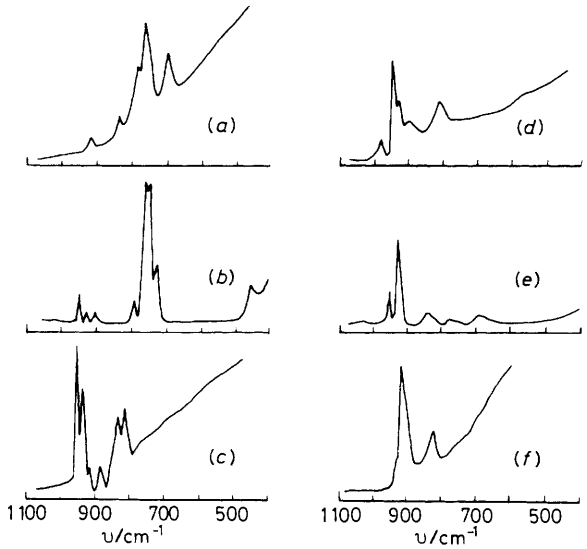

Figure 5. Raman spectra on solid samples of γ-$Ce_2Mo_3O_{13}$ (*a*), β-$Ce_2Mo_3O_{13}$ (*b*), α-$Ce_2Mo_4O_{15}$ (*c*), β-$Ce_2Mo_4O_{15}$ (*d*), $Ce_8Mo_{12}O_{49}$ (*e*), and $Ce_2(MoO_4)_3$ (*f*)

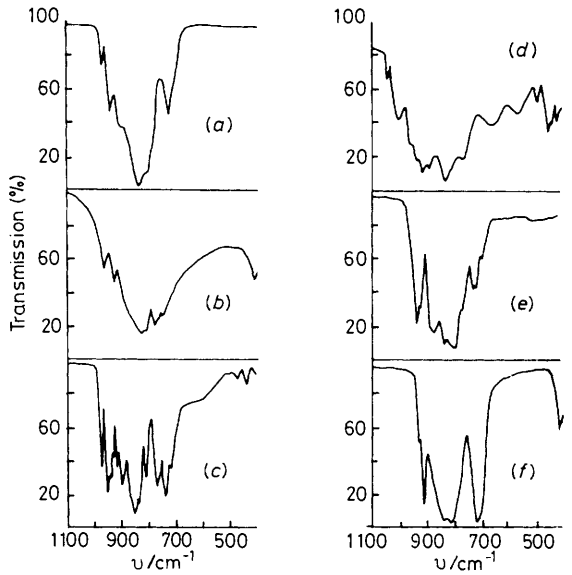

Figure 6. Infrared spectra in KBr pellets of γ-$Ce_2Mo_3O_{13}$ (*a*), β-$Ce_2Mo_3O_{13}$ (*b*), α-$Ce_2Mo_4O_{15}$ (*c*), β-$Ce_2Mo_4O_{15}$ (*d*), $Ce_8Mo_{12}O_{49}$ (*e*), and $Ce_2(MoO_4)_3$ (*f*)

spectrum of $Ce_2(MoO_4)_3$. The ν_1 band at 915 cm^{-1} has become i.r. active as a result of the distortion; the three absorption bands at 845, 815, and 721 cm^{-1} derive from the ν_3 stretching vibration which has lost its degeneracy as a consequence of the decrease in site symmetry. The i.r. spectrum of $Ce_2(MoO_4)_3$ [Figure 6(*f*)] is very similar to that of $Er_2(MoO_4)_3 \cdot nH_2O$, which shows the same number of absorption bands [25] and for which a structure has been advanced with at least C_{2v} symmetry of the MoO_4 tetrahedron. The Raman spectrum of $Ce_2(MoO_4)_3$ does not give further indications about the geometrical distortions; the intense absorption band at 918 cm^{-1} is to be ascribed to the ν_1 stretching vibration and a weaker band at 824 cm^{-1} accounts for one of the three ν_3 derivative bands. The other two absorption bands, which result from the lowering of symmetry of the ν_3 vibration, are probably too weak to be observed in the Raman spectrum.

We conclude that the complexity of the vibrational spectra of the cerium molybdenum oxide compounds in general precludes the presence of a single type of polyhedron [except for $Ce_2(MoO_4)_3$] and is indicative of highly distorted polyhedra (such as octahedra with two very long Mo–O bonds with bond strengths <0.3 v.u.) or mixed-polyhedral types.

Acknowledgements

One of us (J. C. J. B.) is gratefully indebted to the Ramsay Memorial Trust (London) for financial support and to the Department of Metallurgy and Science of Materials, University of Oxford, for generous hospitality.

References

1 N. Ferlazzo and G. Caporali, Ital. P. 749,678/1967.
2 G. Caporali, N. Ferlazzo, and N. Giordano, U.S. P. 3,691,224/1972.
3 N. Giordano and J. C. J. Bart, Proc. Fourth Int. Symposium on Heterogeneous Catalysis, Varna, eds. D. Shopov, A. Andreev, A. Palazov, and L. Petrov, Publication House of the Bulgarian Academy of Sciences, Sofia, 1979, vol. 2, p. 27.
4 M. J. Schwing-Weill, *Bull. Soc. Chim. Fr.*, 1972, 1754.
5 J. C. J. Bart and N. Giordano, *J. Less Common Met.*, 1976, **46**, 17.
6 A. Castellan, J. C. J. Bart, A. Bossi, P. Perissinoto, and N. Giordano, *Z. Anorg. Allg. Chem.*, 1976, **422**, 155.

7 L. H. Brixner, J. F. Whitney, and M. S. Licis Kay, *J. Solid State Chem.*, 1973, **6**, 550.
8 A. M. Golub, V. I. Maksin, and P. Perepelitsa, *Russ. J. Inorg. Chem.*, 1975, **20**, 486.
9 B. M. Gatehouse, Proc. Second Int. Conf. on Chem. and Uses of Molybdenum, eds. P. C. H. Mitchell and A. Seaman, Oxford, 1976, p. 138.
10 J. C. J. Bart and N. Giordano, Ital. P. 1,051,955/1981.
11 R. L. Cohen, G. K. Wertheim, A. Rosencwaig, and H. J. Guggenheim, *Phys. Rev. B*, 1972, **5**, 1037.
12 T. L. Barr, *J. Phys. Chem.*, 1978, **82**, 1801.
13 T. L. Barr, *Am. Lab. (Boston)*, 1978, **10**, 65.
14 T. L. Barr, *Am. Lab. (Boston)*, 1978, **10**, 40.
15 T. L. Barr, 'Electron Spectroscopy for Chemical Analysis Examination of Rare Earths and Near Rare Earth Species,' Quantitative Surface Analysis of Materials, ASTM STP 643, ed. N. S. McIntyre, American Society for Testing and Materials, Philadelphia, 1978, pp. 83—104.
16 K. S. Kim, W. E. Baitinger, J. W. Amy, and N. Winograd, *J. Electron Spectrosc. Relat. Phenom.*, 1974, **5**, 351.
17 T. L. Barr, Proceedings Pittsburgh Conference on Analytical and Applied Spectroscopy, March 1977.
18 A. W. Sleight, B. L. Chamberland, and J. F. Weiher, *Inorg. Chem.*, 1968, **7**, 1093.
19 J. C. J. Bart, F. Cariati, and A. Sgamellotti, *Inorg. Chim. Acta*, 1979, **36**, 105.
20 R. H. Busey and O. L. Keller, *J. Chem. Phys.*, 1964, **41**, 215.
21 G. M. Clark and W. P. Doyle, *Spectrochim. Acta*, 1966, **22**, 1441.
22 G. D. Fallon and B. M. Gatehouse, *J. Solid State Chem.*, 1982, **44**, 156.
23 L. H. Brixner, A. W. Sleight, and M. S. Licis, *J. Solid State Chem.*, 1972, **5**, 247.
24 W. Jeitschko, *Acta Crystallogr., Sect. B*, 1973, **29**, 2074.
25 B. E. Zaitsev, E. I. Zakharikova, B. N. Ivanov-Emin, and G. I. Cherenkova, *Russ. J. Inorg. Chem.*, 1969, **14**, 781.

Received 26*th July* 1982; *Paper* 2/1267